Research Article

Cancer Immunology Research

CD4$^+$ T Cell and NK Cell Interplay Key to Regression of MHC Class I^{low} Tumors upon TLR7/8 Agonist Therapy

Elien M. Doorduijn[1], Marjolein Sluijter[1], Daniela C. Salvatori[2,3], Serenella Silvestri[2,3], Saskia Maas[2,3], Ramon Arens[4], Ferry Ossendorp[4], Sjoerd H. van der Burg[1], and Thorbald van Hall[1]

Abstract

One of the next challenges in cancer immunotherapy is the resistance of tumors to T-cell–based treatments through loss of MHC class I. Here, we show that under these circumstances, the Toll-like receptor (TLR)-7/8 ligand imiquimod, but not the TLR3 ligand poly I:C or TLR9 ligand CpG, mediated an effective antitumor response. The rejection of these immune-escaped cancers was mediated by NK cells and CD4$^+$ T cells, whereas activated CD8$^+$ T cells were dispensable. Application of the innate immune stimulator at a distant site activated NK cells and thereby elicited tumor-specific T-cell responses in tumor-bearing mice. Mechanistically, imiquimod activated NK cells to kill tumor cells, resulting in release of tumor antigens and induction of tumor-specific CD4$^+$ T cells. These T helper cells provoked a strong induction of CXCL9 and CXCL10 in the tumor environment. Simultaneously, imiquimod induced the expression of the cognate chemokine receptor CXCR3 on peripheral lymphocytes. This ignited intratumoral CD4$^+$ T-cell infiltration and accumulation, which was critical for tumor rejection; CXCR3 blocking antibodies mitigated the clinical response. In the effector phase, NK cell recruitment to tumors and their activation depended on CD4$^+$ T cells. Together, we have uncovered a potent immune axis of tumor-specific CD4$^+$ T cells and NK cells that eliminates escaped MHC-I^{low} tumors. *Cancer Immunol Res; 5(8); 642–53. ©2017 AACR.*

Introduction

The field of cancer immunotherapy has made major progress, with the success of immune checkpoint blockades and adoptive T-cell therapies prolonging many lives (1–3). However, not all patients efficiently respond to immunotherapy and ongoing studies are focused on mechanisms of resistance and escape. The next challenge in the field is to elucidate these mechanisms and to find therapeutic approaches that counteract such immune-escaped tumors. An important mechanism through which tumors evade immune recognition is by lowering the expression of MHC class I (MHC-I) molecules that present tumor antigens to cytotoxic T cells, for example, by changing components in the antigen-processing machinery (4–6). This was highlighted in a detailed analysis of tumors from metastatic melanoma patients relapsing after PD-1 treatment (7). Three out of four refractory tumors displayed a defect in the MHC-I antigen presentation due to genetic alterations.

Natural killer (NK) cells are well known for their role in the control of MHC-I^{low} cells, described by the missing-self theory (8, 9). In patients with metastatic melanoma or renal cell carcinoma, adoptive transfer of pre-activated autologous NK cells did not result in effective tumor killing, even though high numbers of transferred cells were maintained in the periphery (10). In mice, several studies exploited the NK cell–sensitive MHC-I^{low} RMA-S tumor, harboring a deficiency in the peptide transporter TAP (9). In a therapeutic setting, outgrowth of RMA-S tumors can be controlled upon adoptive transfer of high numbers of *in vitro* pre-activated NK cells, in combination with severe preconditioning of mice with radiation (11). Outgrowth of these tumors was also delayed by NK cells upon repetitive systemic injection of IL12 and IL18, or with the IL2 "superkine" H9 (12). Thus, NK cells infiltrating RMA-S tumors might display an anergic phenotype, in contrast to NK cells infiltrating RMA tumors (12).

Toll-like receptor (TLR) agonists are frequently used as an adjuvant during vaccination. The single use of TLR agonist has gained increasing interest, with potent effects seen on both innate and adaptive immune cells. In mice, the application of the TLR7-agonist SC-1 resulted in NK cell activation and subsequent tumor control (13). The antitumor effects of different TLR agonists are tested in several clinical trials. These include the treatment of patients with metastatic squamous cell carcinoma of head and neck (SCCHN) with a TLR8 agonist, the use of a TLR2 agonist in non–small cell lung cancer, and that of a TLR9 agonist in metastatic solid tumor (14–16).

[1]Department of Medical Oncology, Leiden University Medical Center (LUMC), Leiden, the Netherlands. [2]Central Laboratory Animal Facility, Leiden University Medical Center (LUMC), Leiden, the Netherlands. [3]Department of Anatomy and Embryology, Leiden University Medical Center (LUMC), Leiden, the Netherlands. [4]Immunohematology and Blood Transfusion, Leiden University Medical Center (LUMC), Leiden, the Netherlands.

Note: Supplementary data for this article are available at Cancer Immunology Research Online (http://cancerimmunolres.aacrjournals.org/).

Corresponding Author: Thorbald van Hall, Leiden University Medical Center, 2333 ZA Leiden, the Netherlands. Phone: 31-71-5266945; Fax: 31-71-5266760; E-mail: T.van_Hall@lumc.nl

doi: 10.1158/2326-6066.CIR-16-0334

In our research on an effective $CD8^+$ T-cell defense for MHC-I^{low} tumors, involving so-called TEIPP antigens (17–21), we found that the TLR7/8 agonist imiquimod induced strong regressions of MHC-I^{low} tumors when applied at distant sites. Imiquimod was applied as Aldara cream, in combination with IL2. Aldara is an FDA- and EMA-approved cream for the treatment of superficial basal cell carcinoma in the skin and genital warts and works by stimulation of the innate immune system. Unexpectedly, Aldara cream effectively induced a complete eradication of established MHC-I^{low} tumors without transfer of NK cells or stringent host preconditioning. Here, we unraveled the underlying mechanisms and show a dominant role for $CD4^+$ T cells and the chemokine receptor CXCR3.

Materials and Methods

Mice and cell lines

The tumor cell lines RMA, RMA-S (TAP2 deficient RMA), B16F10, and B78H1 (MHC-I–deficient B16) have been described before (17, 20). RMA-S and RMA cells were originally derived from Klas Kärre (Karolinska Institutet, Sweden). B16F10 cells were purchased from ATCC and B78H1 cells were a gift from Dr. Iwona Stroynowski (Dallas, Texas, USA). All cells were cultured no longer than 1 month and regularly tested by flow cytometry for MHC class I expression. *Mycoplasma* testing for all cell lines was performed every 2 months by PCR. All cells were cultured in complete IMDM medium (Invitrogen) containing 8% heat-inactivated FCS (Gibco), penicillin (100 U/mL), streptomycin (100 μg/mL) and 2 mmol/L L-glutamine (Invitrogen) at 37°C in humidified air with 5% CO_2. C57BL/6 mice were purchased from Charles River. The TCR transgenic OT2 mice were derived from Jackson Laboratory. The FcγR-deficient mice were provided by Sjef Verbeek (22). Mice were housed in individually ventilated cages and used at 6 to 12 weeks of age. All animal experiments were approved by the ethics committee of the Leiden University Medical Center (LUMC).

Tumor experiments

Female C57BL/6 mice were subcutaneously injected with RMA cells (1×10^6), RMA-S cells (2×10^6), B16 (1×10^5), or B78H1 cells (1×10^6) in 0.1% BSA/PBS (200 μL). At day 5 (RMA, RMA-S) or days 11–12 (B16, B78H1) after tumor challenge, treatment was started on the contralateral flank. For treatment with imiquimod, the flank of the mice was shaved and one-fourth sachet of Aldara (Pharmacy, LUMC) was applied to the shaved skin. To prevent mice from licking the cream, mice were anesthetized with xylazine and ketamine. Other mice got CpG (20 μg; ODN 1826, Invivogen) injected subcutaneously in 200 μL PBS, or 50 μg hiltonol (Oncovir, Inc.) or a 1:1 mixture of PBS/incomplete Freund's adjuvant (IFA) emulsion. All vaccinations were repeated after a week. At the second vaccination and the day after, mice received IL2 (6×10^5 IU) intraperitoneally. Tumor growth was followed and blood was taken from the tail vein to analyze immune cell activation. Mice were sacrificed when the tumor size reached 2,000 mm^3.

In vivo depletions

Cell-type–specific depletion was performed systemically through intraperitoneal injection of one of the antibodies listed in Table 1. To deplete macrophages, mice were given PLX3397 plexxikon chow, containing a tyrosine-kinase inhibitor of CSF-1R (23). Efficiency of the depletions was verified by flow cytometry. To block CXCR3 and IFNAR signaling, specific antibodies were given, as specified in Table 1. A polyclonal Armenian Hamster IgG (BioXcell) and isotype control (SouthernBiotech) were used as controls, respectively.

Immune infiltrate analysis and flow cytometry

For immune infiltrate analyses, mice were sacrificed and the spleen, tumor draining lymph node (dLN), ndLN (mesenteric LN), and tumor were excised. Single-cell suspensions of spleen and lymph nodes were generated by mechanical disruption. The tumor was cut into small pieces that were incubated with liberase (Roche) for 15 minutes at 37°C and then passed over a cell strainer. Cells were washed twice with FACS buffer (0.1% BSA/PBS). To block Fc receptors, cells were incubated with purified CD16/CD32 (clone 2.4G2, BD BioScience) for 15 minutes on ice. Next, cells were washed twice in FACS buffer and stained with the following antibodies: CD4 (clone RM4-5), CD3 (145-C211), CD8 (53-6.7), CD11b (M1/70), CD69 (H1-2F3), Class-II (M5/114.15.2), Ly6C (HK1.4), Gr-1 (RB6-8C5), NK1.1 (PK136), CD11c (HL3), CD45.2 (104), Ly6G (1A8), CD62L (MEL-14), CD44 (IM7), F4/80 (BM8), Siglec-F (E50-2440), CD25 (PC61), CD115 (AFS98), and CXCR3 (CXCR3-173). Dead cells were excluded using 7-AAD. Flow cytometry analysis was done on an LSR Fortessa or FACS caliber (BD Biosciences). Analysis was done in FlowJo software (Tree Star, Inc.). For intracellular cytokine analysis, splenocytes or tumor cells were loaded for 5 hours on 40.000 D1 cells, which had been overnight incubated with the long helper peptide Env-H19 (EPLTSLTPRXNTAWNRLKL), in which a cysteine has been changed to an Abu ("X"; ref. 24) in the presence of GolgiPlug, containing Brefeldin A (BD Biosciences). D1 cells were washed twice to remove any peptide in the medium and cell suspension of spleen or tumor was added to the D1 cells. The minimal epitope GagL (CCLCLTVFL) was added to the cultures at the same time as the Golgiplug. After 5 hours, cells were washed and stained for cell surface markers as described above. Then, cells were fixed and permeabilized using the Intracellular cytokine staining kit (BioLegend) according to manufacturer's protocol. Then, cells were stained for cytokines: IL2 (clone JES6-5H4), IFNγ (XMG1.2), and TNFα (MP6-XT22).

RMA-S cells or B16 cells were treated with IFNγ (BioLegend) or type I IFN (25). After two days, cells were stained with FACS antibodies for H2-D^b (clone 28-14-8), H2-K^b (AF6-88.5), or class-II (M5/114.15.2).

To collect serum, blood was taken from the tail vain, centrifuged for 15 minutes, and serum was collected and stored at −20°C until further use. Cytokines and chemokines from treated mice, which were in sera and in the supernatants of splenocytes that had been cultured overnight on EnvH-loaded D1 cells, were measured using a mouse Bio-Plex Pro Mouse Cytokine 23-plex immunoassay, according to manufacturer's protocol (Bio-Rad).

qPCR analysis

Tumor were isolated, embedded in Tissue-Tek, and frozen in cooled 2-methylbutane. Sections of 20 μm were cut and RNA was isolated from these sections. For *in vitro* stimulated cells, RMA-S cells (0.25×10^6) were plated in a 12-well plate and stimulated for 3 days with IFNγ (100 ng/mL, Biolegend) and/or TNFα (10 ng/mL). $CD4^+$ T cells were isolated from a naïve C57BL/6 mouse and 2×10^6 cells were plated in a 24-well plate and cultured for 2 days with type I IFN or CD3/CD28 antibodies, as

Table 1. Antibodies used for *in vivo* depletions and blocking

Cell type/receptor	Clone	Company	Amount per injection	Frequency
CD4	GK1.5	Own generation[a]	100 μg	Every 6 days
CD8	2.43	Own generation[a]	100 μg	Every 6 days
NK cells	PK136	BioXCell	100 μg	Every 3–4 days
Eosinophils	#238047	R&D systems	15 μg	One day pre- and posttreatment
pDCs	120G8	Own generation[a]	250 μg	One day pre- and posttreatment
Granulocytes	RB6-8C5	Own generation[a]	300 μg	One day pre- and posttreatment
CXCR3	CXCR3-173	BioXCell	200 μg	Every 3 days Start day 4 (tumor outgrowth) or day 7 (intratumoral analysis)
IFNAR	MAR1-5A3	BioXCell	750 μg	One day pre- and posttreatment

[a]Antibodies were generated as described before (23).

described (21). Then, cells were harvested, washed twice with PBS, and RNA was isolated using the RNeasy Kit (Qiagen) according to manufacturer's protocol. cDNA was synthesized using the High capacity RNA-to-cDNA Kit (Applied Biosystems) according to manufacturer's protocol. qPCR analyses were performed using the SybrGreen supermix (Bio-Rad). Ct values were normalized to the expression levels of housekeeping genes GAPDH and/or YWHAZ. Primer sequences are listed in Table 2.

Immunohistochemistry

Paraffin-embedded and formalin-fixed sections were stained for CD4 antigen using citric buffer antigen retrieval (pH 6) and rabbit monoclonal antibody to CD4 (50134-R001-50, Sino Biological Inc.). Sections were incubated with the biotinylated secondary antibody (goat anti-rabbit IgG; BA-1000, Vector Laboratories, Inc.), followed by the Vectastain ABC Kit (PK-4000, Vector Laboratories, Inc.), as chromogen 3,3′-diaminobenzidine (DAB) was used.

Statistical analysis

Statistical analyses were performed using GraphPad Prism, version 6.0. In tumor experiments, Kaplan–Meier survival curves of mice were analyzed using the log-rank (Mantel–Cox) assay. Additional statistical methods are described in the figure legends. P values < 0.05 were considered statistically significant.

Results

Involvement of NK cells in Aldara-induced MHC-I^{low} tumor regression

In our search for a strong innate stimulus that could support T-cell responses, we observed that the imiquimod-containing cream Aldara induced a robust antitumor response to the MHC-I^{low} tumor RMA-S (Fig. 1A). Aldara was applied twice topically on the contralateral skin and IL2 was given at the second application of the cream. This led us to compare this therapeutic effect with that of other vaccine adjuvants on established RMA-S tumors. Mice receiving saline or incomplete Freunds adjuvants (IFA) at the contralateral flank had to be sacrificed within 15 days due to progressive tumor burden (Fig. 1A and B). Treatment with TLR9 ligand CpG or TLR3 ligand Hiltonol resulted in a modest delay of tumor outgrowth, but tumors grew progressively and all mice needed to be sacrificed after about 20 days. In contrast, all Aldara-treated mice showed regression and active elimination of established tumors. All mice survived at least up to 45 days (Fig. 1B). To determine the contribution of the TLR7/8 ligand imiquimod and the cytokine IL2 in this combination treatment, we treated mice with these agents separately. Injection of IL2 alone did not display any impact on tumor growth and Aldara application showed partial control, whereas the combination of the two induced better tumor regression (Supplementary Fig. S1A). Thus, only the combination led to active elimination of MHC-I^{low} tumors at distant sites.

Aldara application induces high production of systemic type I IFN, and we therefore measured an array of cytokines and chemokines that could be released in a cascade (26). Two days after treatment, no IFNα could be detected in sera from treated mice, indicating that this cytokine was quickly removed from the system. As shown before, CXCL1, G-CSF and IL1α, concentrations were increased, as well as IL10, IL12(p40), CCL2, CCL3, CCL4 and RANTES. (Fig. 1C; refs. 13, 26). Five days after treatment, all cytokines were back to baseline, except TNFα. No elevated concentrations of IL6, IL17, or IFNγ were observed. We concluded that the application of Aldara induced a brief cytokine-release syndrome, but no severe toxicities. Immunohistochemical assessment of tissues confirmed this conclusion.

Next, the same treatment protocol was applied to mice bearing the related RMA tumor line, expressing high levels of MHC-I and therefore insensitive to NK cell–mediated killing (8, 9, 27). Tumor regressions were observed only rarely when MHC-I^{high} RMA-bearing mice were treated with Aldara cream (Fig. 1D). These results indicated a possible role for NK cells.

Imiquimod is a TLR7/8 ligand and induces type I IFN when applied in mice, leading to systemic activation of lymphocytes (13, 28–30). To assess the capacity of the tested adjuvants on lymphocyte activation in the system, we analyzed the frequency and activation status of T cells and NK cells. No differences in the frequencies of circulating T cells were detected between adjuvants

Table 2. Primer sequences for qPCR

Gene	Forward (5′–3′)	Reverse (5′–3′)
GAPDH	GTGCTGAGTATGTCGTGGAGTCTAC	GGCGGAGATGATGACCCTTTTGG
YWHAZ	AAGACAGCACGCTAATAATGC	TTGGAAGGCCGGTTAATTTTC
CXCL9	TGGAGTTCGAGGAACCCTAGT	AGGCAGGTTTGATCTCCGTT
CXCL10	ACGAACTTAACCACCATCT	TAAACTTTAACTACCCATTGATACATA
CXCL11	AGGAAGGTCACAGCCATAGC	CGATCTCTGCCATTTTGACG
CCL2	CGGAACCAAATGAGATCAGAACCTAC	GCTTCAGATTTACGGGTCAACTTCAC

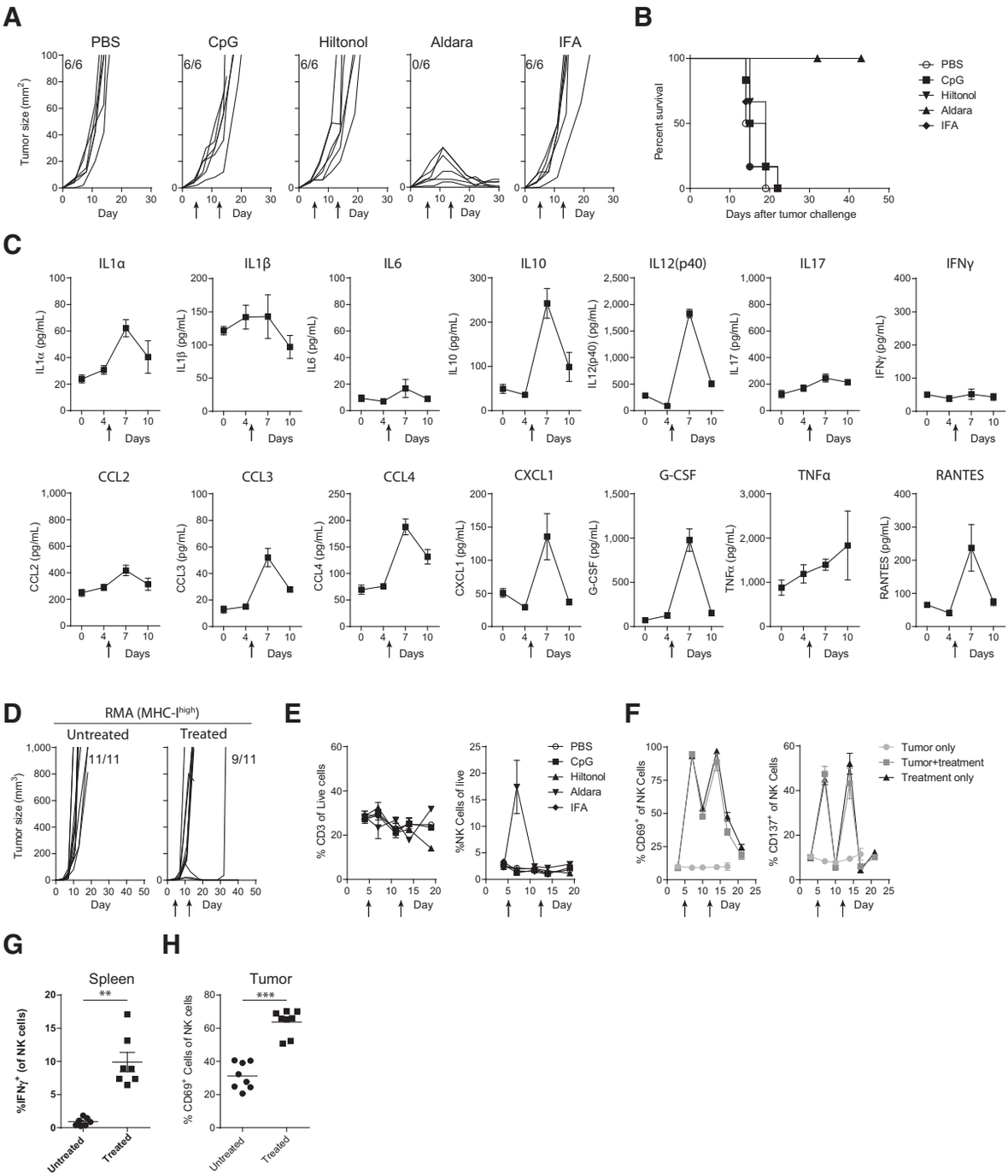

Figure 1.

Imiquimod-containing cream Aldara efficiently controls RMA-S tumors. **A** and **B,** Mice were inoculated with 2×10^6 RMA-S cells subcutaneously. Five days later, when a palpable tumor was present, treatment was started on the contralateral flank (indicated by arrow). Mice received either PBS, CpG, Hiltonol (polyI:C), $^1/_4$ sachet of Aldara cream or incomplete Freud's adjuvant (IFA). Tumor size was measured over time. Data are shown from two independent experiments with 3 mice per group. **B,** Kaplan–Meier survival curves. **C,** Serum of Aldara-treated tumor-bearing mice was collected and analyzed for the presence of several cytokines. Three mice per group, shown as mean and SEM. **D,** Mice were inoculated with 1×10^6 RMA cells and at day 5 after tumor challenge, treatment was started with Aldara cream on the contralateral flank. Data from three independent experiments with 3–5 mice per group. **E,** Blood was taken twice a week from the different treatment groups and analyzed by flow cytometry for the presence of various immune cell subsets. Data are shown from one experiment as mean and SEM with 3 mice per group. **F,** Blood was taken from mice bearing RMA-S tumor alone, Aldara treatment alone, or combination of both tumor and treatment. Data are shown as mean and SEM from one experiment with 2–3 mice per group. **G,** Seven days after tumor challenge, spleens of mice were harvested and an ICS was performed. **H,** The phenotype of intratumoral NK cells in untreated and treated mice was analyzed by flow cytometry at day 11 after tumor challenge. Shown are pooled data from two independent experiments with 3–4 mice per group. Student *t* test, **, $P < 0.01$; ***, $P < 0.001$.

tested in tumor-bearing mice (Fig. 1E). In contrast, NK cell frequency increased briefly in Aldara-treated mice (Fig. 1E). No other adjuvant induced increased NK cell frequencies in blood, suggesting that NK cells were important for tumor rejection. Additionally, Aldara treatment led to NK cell activation as measured by CD69 upregulation (Supplementary Fig. S1B). CpG, and to a lesser extent hiltonol, could activate NK cells in treated mice, but did not increase their numbers (Supplementary Fig. S1B and Fig. 1E). The presence of MHC-I^{low} tumors did not influence NK cell activation, as Aldara application to the skin of naïve mice resulted in similar activation (Fig. 1F, for CD69 and CD137).

The strong activation and increased frequency of NK cells induced after the first application of Aldara, without addition of IL2, was most likely the result of systemic release of type I IFN. Indeed, a clear increase in the frequency of myeloid cells was also detected in blood, mainly CD11b$^+$Ly6G$^+$ neutrophils, in line with a study in which Aldara induced S100A8/9 and CXCL1, as we also observed in serum of treated mice (Fig. 1C), which mediates neutrophil mobilization (Supplementary Fig. S1C; ref. 26). The involvement of NK cells in the Aldara-driven reduction of tumor mass was supported by the proportion of NK cells in spleen (Fig. 1G), and to a lesser extent the tumors (Supplementary Fig. S1D), of treated mice that produced the antitumor cytokine IFNγ. Additionally, tumor-infiltrating NK cells in treated mice had significantly increased expression of CD69, when compared with untreated tumors (Fig. 1H). Finally, NK-sensitive mouse melanomas B16F10 and B78H1 also responded to Aldara treatment (Supplementary Fig. S1E and S1F). These results show that a brief treatment of Aldara with IL2 could effectively activate NK cells and had clinical effects on established NK-sensitive tumors present at distant sites.

CD4$^+$ T cells are indispensable for antitumor effect

The increased frequency of NK cells and their activated phenotype shortly after Aldara treatment, combined with the lack of tumor control in RMA tumor-bearing mice, suggested that NK cells were involved in the regression of RMA-S tumors. Consistent with previous studies (9, 11), antibody depletion of NK cells initially increased tumor size (Fig. 2A and B) but the majority of tumors still regressed at later time points. However, the antibody-mediated depletion of NK cells was incomplete during Aldara treatment (Supplementary Fig. S2A), most likely due to the vigorous TLR triggering and high concentrations of type I IFN, thereby underestimating the role for NK cells (28). Depletion of

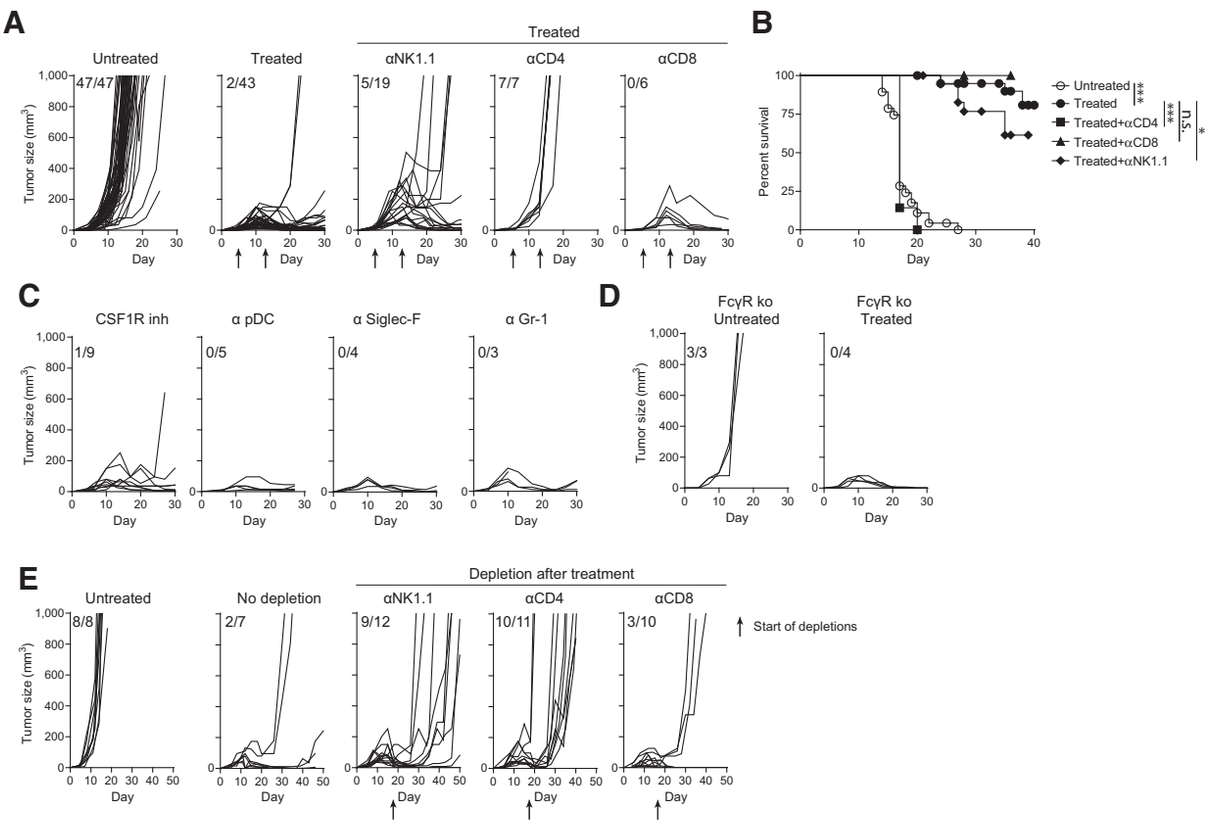

Figure 2.

CD4$^+$ T Cells are indispensable for tumor eradication by Aldara Cream. RMA-S tumor bearing mice were treated with Aldara. Different immune cell subsets were depleted prior to tumor inoculation. **A,** Tumor outgrowth. **B,** Kaplan–Meier survival curves for different depletion groups. Data are shown from at least two experiments with 3–5 mice per group. Log-rank (Mantel–Cox), n.s., nonsignificant, *, $P < 0.05$; ***, $P < 0.001$. **C,** Different myeloid cell populations were depleted. Data are shown from one or two experiments with 3–5 mice per group. **D,** Mice deficient for all Fcγ receptors were inoculated with RMA-S tumors, treated with Aldara and tumor outgrowth was followed. Data from one experiment with 3 or 4 mice per group. **E,** Depletion was started after successful tumor regressions, at day 18. Arrow indicates start of depletion. Data are pooled from two independent experiments with 4–8 mice per group.

$CD8^+$ T cells did not affect tumor treatment, as expected from the low MHC-I expression on the tumors (Fig. 2A and B). Depletion of $CD4^+$ T cells, however, completely abrogated the antitumor effect of Aldara (Fig. 2A and B). Tumors in Aldara-treated, $CD4^+$ T-cell–depleted mice grew out at comparable rates as untreated mice, emphasizing the crucial role the $CD4^+$ T cells had in the antitumor effect upon treatment.

RMA-S cells cannot be killed directly by $CD4^+$ T cells, because they lack MHC class II (MHC-II) expression, even after cytokine stimulation (Supplementary Fig. S2B and C). So other cell types, in addition to NK cells, could be involved in the tumor cell killing *in vivo*. Eosinophils and macrophages can mediate killing of MHC-II^{low} tumors (31, 32). To examine the role of various myeloid cell types, we depleted several around the time of treatment, including tissue-resident $CSF1R^+$ macrophages, plasmacytoid dendritic cells (pDC), eosinophils, and neutrophils. None of these myeloid cell subsets were involved in the antitumor response (Fig. 2C). Antibody-dependent cellular cytotoxicity (ADCC) was examined with mice lacking all Fcγ receptors. Treatment with Aldara resulted in comparable tumor regressions as in wild-type mice (Fig. 2D). Thus, the antitumor effect of Aldara on RMA-S tumors did not depend on eosinophils, tissue-resident macrophages, pDCs, granulocytes, or ADCC.

To investigate whether type I IFN is involved in effective tumor control, mice were given antibodies to block the IFNAR receptor. At day 17 after tumor inoculation, mice treated in the presence of the IFNAR blocking antibody had significantly larger tumors than treated mice (Supplementary Fig. S2D), supporting the involvement of type I IFN.

Most Aldara-treated tumors completely regressed and were no longer palpable, whereas others remained very small for several weeks. To determine whether $CD4^+$ T cells and NK cells were involved in the active control of these residual tumor lesions, we depleted specific cell types starting at day 18 after tumor challenge, when tumors had successfully regressed after treatment. Upon depletion of $CD4^+$ T cells or NK cells, nearly all tumors grew out again and mice had to be sacrificed due to progressive tumor burden (Fig. 2E; Supplementary Fig. S2D). Thus, both $CD4^+$ T cells and NK cells were crucial for keeping small tumors in an immune-mediated state of equilibrium. $CD8^+$ T-cell depletion had no effect, similar to their depletion at the acute phase of treatment.

In conclusion, we observed a crucial role for tumor growth control by $CD4^+$ T cells both during and after Aldara-mediated regressions of RMA-S tumors, indicative for immune-mediated tumor senescence.

Strong influx of $CD4^+$ T cells in the tumor upon treatment

We studied the intratumoral immune cell composition in more detail. Mice were sacrificed at day 14 (early) or day 18 (late) after tumor inoculation and immune cell infiltrates were analyzed by flow cytometry (Fig. 3A). The frequency of intratumoral $CD4^+$ T cells increased 5-fold after treatment; from 5% of infiltrating immune cells in untreated tumors to up to 25% in treated tumors at day 18 (Fig. 3B). The intratumoral frequency of $CD8^+$ T cells also increased after treatment, but did not accumulate over time (Fig. 3B). The frequency of intratumoral NK cells was relatively low in untreated tumors ($3.9\% \pm 0.4\%$) and did not significantly increase upon treatment from day 14 onward. The relative infiltration of myeloid cells reduced over time, presumably reflecting increased infiltration of $CD4^+$ T cells, as all frequencies were calculated as relative proportions of all $CD45^+$ immune cells. Within the myeloid cell compartment, there was a temporal increase in the neutrophil population, as shown before in blood, and a drop in macrophages over time (Supplementary Fig. S3A). These shifts in T-cell composition were specific for the tumor environment and were not observed in spleens or tumor-draining lymph nodes (dLN; Fig. 3C; Supplementary Fig. S3A and S3B). Aldara treatment, therefore, led to a strong and selective influx of $CD4^+$ T cells in the tumor within days after treatment.

To verify that the increased $CD4^+$ T-cell infiltrate did not reflect a drop in another cell population, we performed immunohistochemistry analysis. After one application of Aldara, at day 11 after tumor inoculation, $CD4^+$ T-cell infiltration increased (Fig. 3D). Multifocal clusters of $CD4^+$ T cells were visible at the tumor burden and in the center of the tumor (Fig. 3D). In untreated tumors, few intratumoral $CD4^+$ T cells were detected in stroma or tumor beds. This was in line with our flow cytometry analysis and confirmed a strong $CD4^+$ T-cell influx.

We determined the phenotype of intratumoral $CD4^+$ T cells. As expected, most intratumoral $CD4^+$ T cells had an activated phenotype ($CD62L^{low}CD44^{high}$), even in untreated mice (Supplementary Fig. S3C). More than 60% of tumor-infiltrating $CD4^+$ T cells in Aldara-treated mice expressed T-bet, a marker delineating Th1 cell function, whereas less than 20% of intratumoral $CD4^+$ T cells from untreated mice expressed it (Fig. 3E). Thus, the treatment protocol induced the intratumoral accumulation of activated Th1 $CD4^+$ T cells.

Tumor-specific $CD4^+$ T cells drive the tumor rejection response

Although the Aldara cream activates innate immunity, the increased infiltration of activated Th1 $CD4^+$ T cells implies the induction of adaptive immunity and specific responses. The MHC-I^{low} RMA-S cell line expresses a murine leukemia virus (MuLV) Env "helper"-epitope that is a tumor-specific antigen in this model (24). Indeed, circulating EnvH-specific $CD4^+$ T cells were expanded after the second application of Aldara (Fig. 4A and B) and their frequencies increased steadily over time to reach 1% of total $CD4^+$ T cells in blood 3 weeks after the start of treatment (Fig. 4C). The T-cell response was EnvH-specific, because the T cells did not respond to a control peptide during the *ex vivo* analysis (Supplementary Fig. S4A). No circulating EnvH-specific T cells were detected in untreated tumor-bearing mice or in Aldara-treated, non–tumor-bearing mice (Fig. 4C). Thus, both RMA-S tumor antigens and treatment with Aldara were required for the induction of tumor-specific $CD4^+$ T cells, in contrast to NK cell induction, which did not rely on the tumor being present (Fig. 1). So, an innate stimulus can lead to the presence of tumor-specific $CD4^+$ T cells in RMA-S tumor–bearing mice.

Tumor-specific $CD4^+$ T cells were also present in tumor lesions. Tumors were harvested at day 18 after tumor challenge, mechanically disrupted, and a single-cell suspension was stimulated for 5 hours with EnvH-peptide–loaded dendritic cells. In tumors of treated mice, up to 10% of $CD4^+$ T cells produced both IFNγ and TNFα when stimulated with EnvH peptide-loaded cells (Fig. 4D). When these cell suspensions were stimulated with non-loaded cells, already 3%–4% of $CD4^+$ T cells produced both cytokines, probably as a consequence of tumor-derived antigen present in the cell suspensions. Additionally, intratumoral $CD4^+$ T cells in treated mice produced IL2 (Fig. 4D). Peripheral tumor-specific $CD4^+$ T cells in treated mice also produced IL4, IL6, IL10, IL13, and GM-CSF when stimulated with their specific peptide

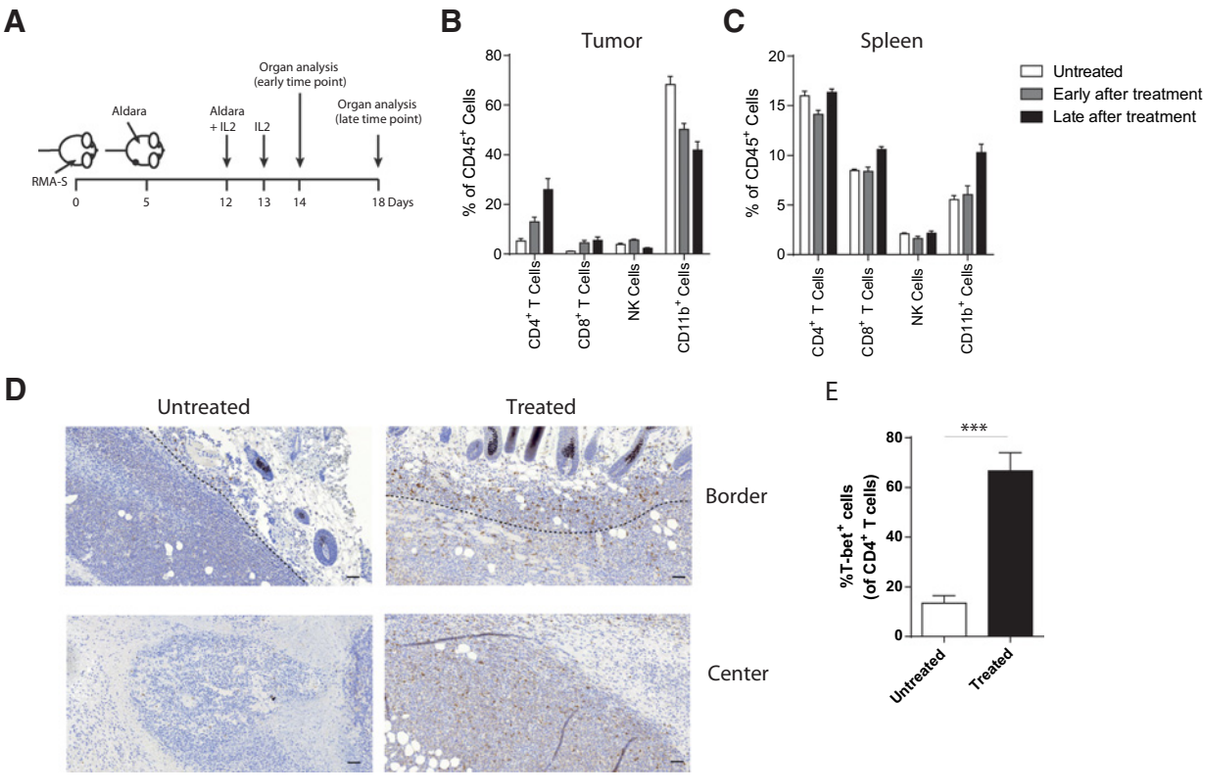

Figure 3.

Increased infiltration of $CD4^+$ T cells in Aldara-treated tumors. Tumor-bearing mice were treated with Aldara and early (day 14) or late (day 18) after tumor inoculation, tumor and lymphoid organs were analyzed. As a control, untreated mice were used, bearing comparable sizes of tumors. **A,** Schematic overview. **B** and **C,** Frequency of $CD4^+$ T cells, $CD8^+$ T cells, NK cells, or $CD11b^+$ cells within the $CD45^+$ population, in tumor (**B**) or spleen (**C**). Data are shown as mean with SEM and are pooled from two or three experiments with 3 mice per group. **D,** Tumors were dissected at day 11 after tumor inoculation and immunohistochemic analysis was performed using a CD4-specific antibody. One of three mice is shown. Scale bar, 50 μm. **E,** The phenotype of intratumoral $CD4^+$ T cells was analyzed by flow cytometry at day 18 after tumor inoculation. Pooled data are shown as mean with SEM and from two independent experiments with 3 mice per group. Student *t* test, ***, $P < 0.001$.

(Supplementary Fig. S4B). In contrast, T cells from untreated tumors stimulated with peptide-loaded DCs had no increase in cytokine-producing $CD4^+$ T cells (Fig. 4D). Thus, this form of immunotherapy resulted in an intratumoral influx and enrichment of tumor-specific $CD4^+$ T cells that produced a broad spectrum of cytokines.

We also analyzed the induction of tumor-specific $CD8^+$ T cells. Even though these cells were not critical for tumor elimination (Fig. 2), $CD8^+$ T cells specific for the immunodominant epitope from the Gag protein of the MuLV virus presented by these tumor cells (24) were present in spleens and tumors of successfully treated mice (Supplementary Fig. S4C and S4D). This suggests that the release of antigen primes tumor-specific $CD8^+$ and $CD4^+$ T cells, available for tumor attack, but that the low expression of MHC-I on the RMA-S tumor renders $CD8^+$ T cells ineffective.

Because Aldara cream upregulated CD69 on $CD4^+$ and $CD8^+$ T cells (Supplementary Fig. S4E), we wanted to validate the relevance for tumor-specificity of $CD4^+$ T cells or whether any $CD4^+$ T cell activated upon Aldara treatment could induce tumor regressions. To this end, we performed the same treatment experiment in TCR-transgenic OT-II mice, in which all $CD4^+$ T cells are specific for an ovalbumin epitope and, as a consequence, fail to induce tumor-specific $CD4^+$ T cells in this model. There was a complete lack of treatment efficacy in these mice (Fig. 4E). The increased NK cell frequency and activation in OT-II mice was comparable with that of treated B6 mice (Fig. 4F). The tumor-specificity of the $CD4^+$ T cells was crucial for tumor eradication and only NK cell activation by Aldara was not sufficient.

Impact of $CD4^+$ T-cell depletion on intratumoral immune cell composition

To better understand the underlying mechanism of tumor eradication, the immune cell composition as well as chemokine profile in $CD4^+$-depleted tumors were analyzed. The frequency of tumor-infiltrating $CD8^+$ T cells in $CD4^+$ T cell–depleted mice was increased, corresponding to the absence of the $CD4^+$ T-cell population (Fig. 5A). The intratumoral NK cell population in $CD4^+$ T-cell–depleted tumors significantly decreased (Fig. 5A). However, the frequency of NK cells in spleens of $CD4^+$ T-cell–depleted mice not reduced (Fig. 5B), suggesting that tumor-specific $CD4^+$ T cells actively recruited NK cells to the tumor site. Within the myeloid cells of the tumor, neutrophils increased slightly, whereas eosinophil frequency was significantly reduced upon Aldara treatment, and trended downward again upon $CD4^+$ T-cell depletion. The residual NK cells in $CD4^+$ T-cell–depleted tumors had significantly reduced expression of the activation

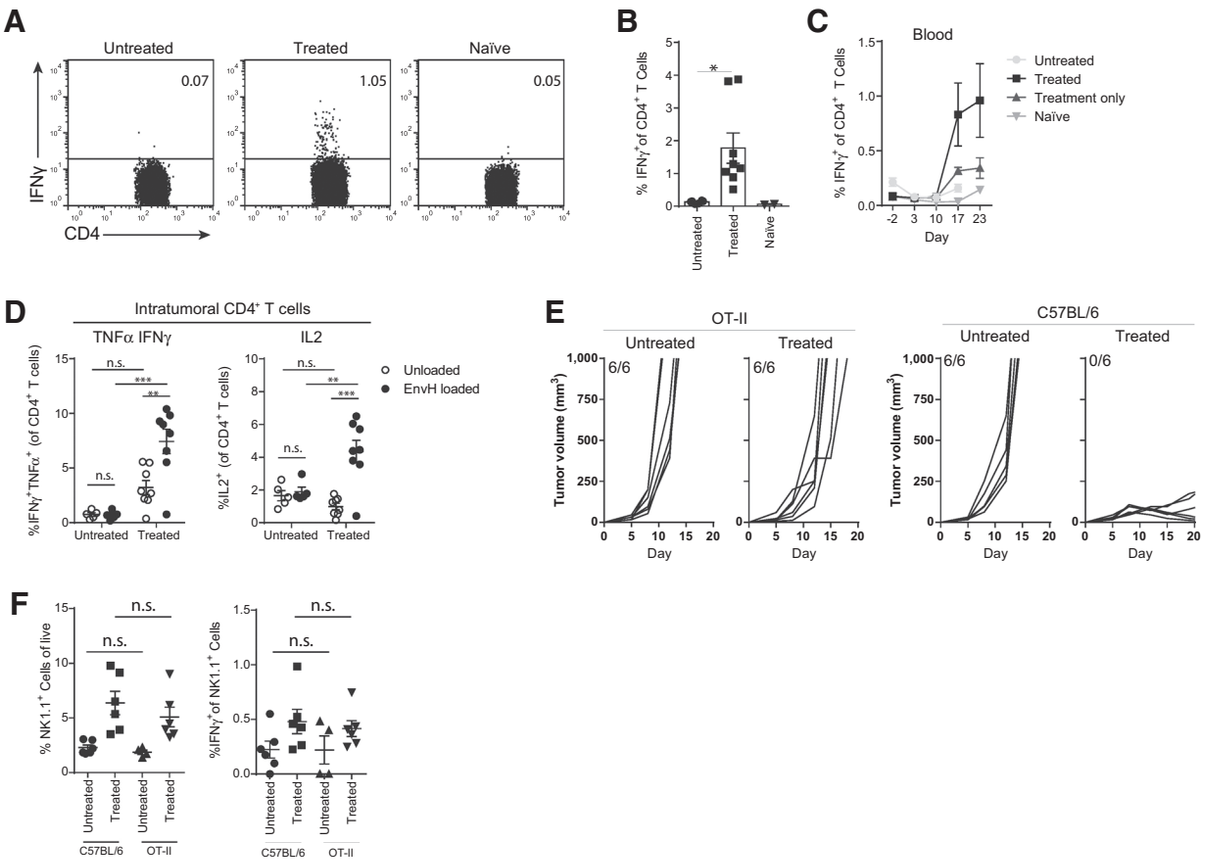

Figure 4.

Tumor-specific CD4$^+$ T cells are required for RMA-S eradication. **A** and **B,** Blood was taken at day 17 after tumor inoculation from untreated, treated, or naïve mice and was cultured overnight with the long EnvH peptide. The next day, an ICS was performed. Data representative for at least two independent experiments and plots are gated on CD4$^+$ T cells. **C,** Blood was taken from mice with only tumor, treatment only, treatment and tumor or naïve and an ICS was performed to analyze cytokine production by CD4$^+$ T cells. Data represent mean + SEM and shown are five mice per group. **D,** Cytokine production by intratumoral CD4$^+$ T cells was measured by ICS at day 18 after tumor inoculation. Data are pooled from three independent experiments with three mice per group. Two-way ANOVA. **, $P < 0.01$; ***, $P < 0.001$, n.s., nonsignificant. **E,** OT-II TCR transgenic mice were inoculated with RMA-S tumor cells and treated with Aldara cream as before. Data from one experiment with 6 mice per group. **F,** Blood was taken from B6 or OT-II transgenic mice at day 15 after tumor inoculation and analyzed by flow cytometry. Student *t* test, *, $P < 0.05$; n.s., nonsignificant.

receptor NKG2D (Fig. 5C), yet KLRG1 was induced by treatment and not reduced in CD4$^+$ T-cell–depleted animals (Fig. 5D).

The significantly reduced frequency of intratumoral NK cells in CD4$^+$ depleted mice, together with their importance in RMA-S eradication, prompted us to investigate chemokine expression profiles in homogenized tumors. In treated tumors, IFNγ-induced chemokine CXCL10 was significantly elevated, described to be involved in the attraction of NK cells to sides of infections and tumors (Fig. 5E; refs. 33–35). Neither CXCL11 nor the inflammatory macrophage attractant CCL2 increased in treated tumors (Fig. 5E). Removal of CD4$^+$ T cells significantly reduced expression of CXCL10, but did not affect the levels of the other chemokines (Fig. 5E). This indicates that the intratumoral expression of CXCL10 was induced by tumor-infiltrating CD4$^+$ Th1 cells and this could mediate NK cell recruitment to the tumor, as previously suggested (33, 34). RMA-S tumor cells produced high mRNA levels of CXCL10 after *in vitro* stimulation with IFNγ, which was further increased when TNFα was added (Fig. 5F). Expression of CXCL9 or CXCL11 was not induced by these two cytokines, indicating that the CXCL9 measured in tumor lysates was produced by other cells in the tumor such as myeloid cells. Additionally, CD4$^+$ T cells also upregulated CXCL10 when stimulated *in vitro* with type I IFN (Supplementary Fig. S4F). Therefore, intratumoral CD4$^+$ Th1 cells stimulated the release of CXCL10 by tumor cells and other immune-infiltrating cells.

T-cell influx, but not NK cells, depends on CXCR3 signaling

NK cells are attracted to sites of infection and to tumors by chemokines CXCL9 and CXCL10 (33–35), so we assessed NK cell migration in the presence of an antibody against the cognate chemokine receptor CXCR3. Mice receiving the blocking antibody to CXCR3 displayed no change in their frequency of intratumoral NK cells (Fig. 6A). However, intratumoral CD4$^+$ T-cell accumulation instigated by Aldara cream was completely lost in these mice after anti-CXCR3 treatment (Fig. 6B). Thus, the tumor infiltration of CD4$^+$ T cells after treatment completely depended on CXCR3 signaling, whereas NK cell infiltration of RMA-S tumors was independent of this receptor.

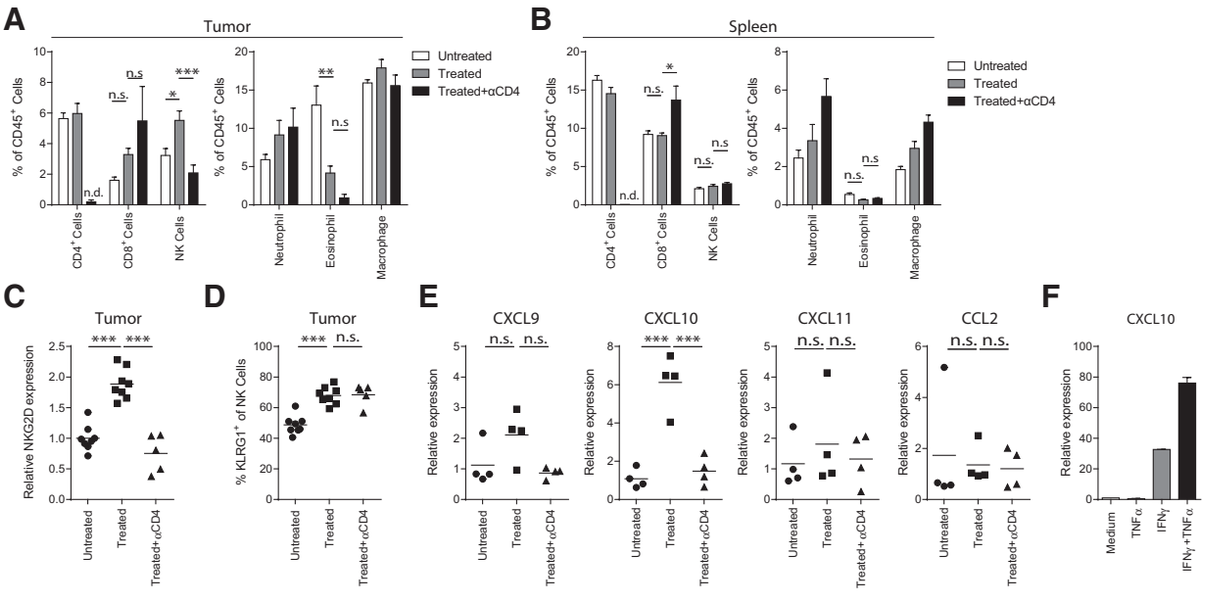

Figure 5.

Reduced NK cell infiltrate and CXCL9/10 levels in $CD4^+$ T cell–depleted tumors. **A** and **B,** Tumor-bearing mice were depleted of $CD4^+$ T cells and frequencies of immune cell subsets were analyzed by flow cytometry at day 11 after tumor inoculation, in tumor (**A**) and spleen (**B**). Data are pooled from two or three independent experiments with three mice per group and shown as mean + SEM. **C** and **D,** Mean fluorescent intensity of NKG2D (**C**) and KLRG1 expression (**D**) on intratumoral NK cells, at day 11 after tumor inoculation. Data pooled from two independent experiments with 4 mice per group. **E,** Tumors were dissected at day 7 after inoculation and qPCR analysis was done for various chemokines. Expression levels are normalized for household genes and untreated tumors. Data from one of two qPCRs with four mice per group. **F,** Expression level of CXCL10 by RMA-S cells upon *in vitro* stimulation with IFNγ and/or TNFα. Data are representative for one of two independent experiments. One-way ANOVA; n.s., nonsignificant; *, $P < 0.05$; **, $P < 0.01$; ***, $P < 0.001$.

In naïve mice, the CXCR3 receptor was expressed on about 15% to 20% of circulating NK cells (Fig. 6C and D). In untreated, tumor-bearing mice, this frequency did not change. Upon treatment with Aldara, the frequency of $CXCR3^+$ NK cells nearly doubled, so the lack of CXCR3 blocking effect was not related to absence of the receptor. In contrast, the frequency of circulating $CXCR3^+$-expressing T cells increased almost 10-fold for $CD4^+$ T cells and 3-fold for $CD8^+$ T cells (Fig. 6C and D). These frequencies were much higher than that of antigen-specific cells, suggesting that the TLR7 ligand imiquimod can drive migration of T cells even in the absence of priming. These data imply that the infiltration of NK cells to the tumor is independent of CXCR3-CXCL9/10 signaling, but is mediated via a yet unknown $CD4^+$ T-cell–mediated axis. So, the influx of $CD4^+$ T cells operates by a self-perpetuating system involving IFNγ-CXCL10-CXCR3, and is ignited by Aldara.

Finally, we examined if CXCR3 signaling was essential for the treatment efficacy by Aldara and IL2. Treatment was not effective in most mice that received the CXCR3 blocking antibody. Tumors grew out and most mice had to be killed due to tumor burden (Fig. 6E and F). In contrast, mice receiving an isotype control antibody responded well to treatment, with most the tumors regressed and tumors effectively controlled (Fig. 6E and F). Despite the relative frequency of intratumoral NK cells remaining unchanged in mice that received the CXCR3 blocking antibody, this did not result in effective tumor control, indicating that intratumoral $CD4^+$ T cells were required for additional stimulation. Thus, tumor-specific $CD4^+$ T cells and CXCR3 signaling are pivotal in the Aldara-mediated control of RMA-S tumors.

Discussion

In this study, we unraveled a previously unknown interplay of $CD4^+$ T cells with NK cells involved in the clearance of the aggressive RMA-S tumor, which has low MHC-I expression and no MHC-II. Active tumor regressions were induced by two applications of the imiquimod-containing cream Aldara at a distant site, and completely depended on both the induction of tumor-specific $CD4^+$ T cells and NK cells. NK cells were activated upon Aldara application and, most likely, initiated the killing of tumor cells. This resulted in the release of necessary tumor antigens for priming of tumor-specific $CD4^+$ T cells. The intratumoral $CD4^+$ T cells subsequently induced the expression of CXCL10 and together with the upregulated expression of the CXCR3 receptor on lymphocytes created a positive feedback loop in which more $CD4^+$ and $CD8^+$ T cells infiltrated the tumor. Activated $CD4^+$ T cells of the Th1 type then recruited more NK cells to the tumor, eventually resulting in tumor regressions of established cancers. Furthermore, both $CD4^+$ T cells and NK cells maintained tumors under immune-mediated control after successful treatment.

Whereas induction of tumor-specific $CD4^+$ T cells depended on the presence of tumors and Aldara, peripheral NK cells were activated by Aldara alone. Even though they were essential to tumor regression, the frequency of intratumoral NK cells was low. Upon treatment, this frequency slightly increased, but still remained a relatively small fraction of the immune cell infiltrate. Homing of NK cells to the tumor depended on the presence of $CD4^+$ T cells, but did not require signaling by CXCR3. This is in contrast to what was reported by others (33, 34). We presume that

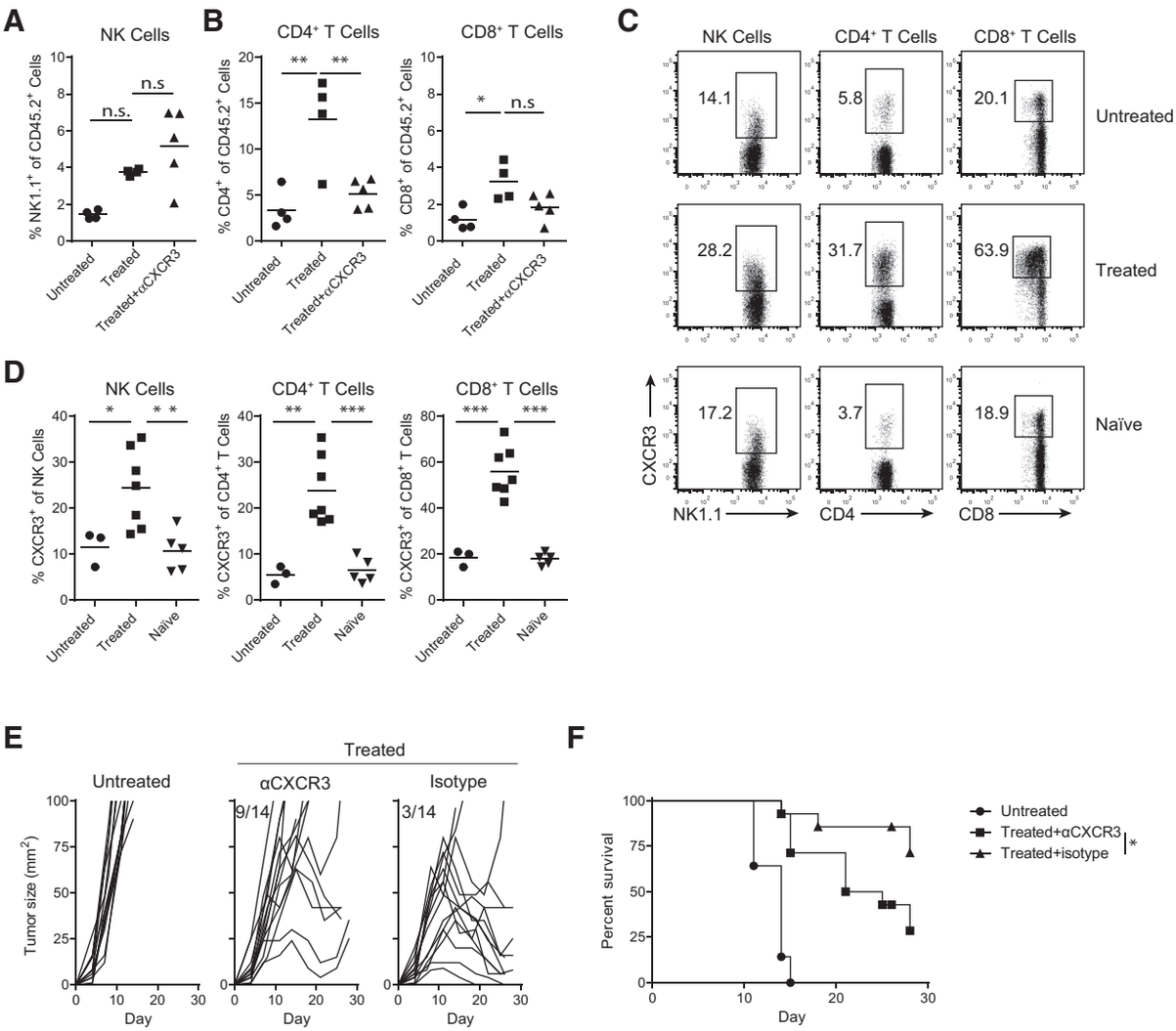

Figure 6.

CXCR3 signaling involved in Aldara-mediated tumor effect. **A** and **B,** Intratumoral frequencies of NK cells (**A**) and CD4$^+$ and CD8$^+$ T cells (**B**) in untreated, treated, or treated mice receiving CXCR3 blocking antibody, analysis at day 15 after tumor inoculation. Data are pooled from two independent experiments with 2–3 mice per group (one-way ANOVA; n.s., nonsignificant, *, $P < 0.05$; **, $P < 0.01$). **C** and **D,** Expression of CXCR3 levels was measured by flow cytometry at day 4 after second Aldara treatment. Data are shown from two independent experiments. Student *t* test, *, $P < 0.05$; **, $P < 0.01$; ***, $P < 0.001$. **E** and **F,** Tumor outgrowth of RMA-S tumor–bearing mice, untreated, treated combined with CXCR3 blocking antibody or isotype control. Data from two independent experiments with 6–8 mice per group. Log-rank (Mantel–Cox), *, $P < 0.05$.

other chemokines from CD4$^+$ T cells are involved in NK cell recruitment to the tumor, such as CCR2, CCR5, or CX3CR1 (36).

Neutralization of CXCR3 in Aldara-treated mice prevented CD4$^+$ T-cell influx and resulted in tumor outgrowth in the majority of cases, despite the presence of intratumoral NK cells. This suggests that NK cells required additional signals from the adaptive lymphocytes to efficiently kill tumor cells. This is in line with the reduced NKG2D expression by NK cells in CD4$^+$ T-cell–depleted tumors. Intratumoral CD4$^+$ T cells in treated mice produced TNFα, IFNγ, and IL2 and we hypothesize that these cytokines are needed for optimal activation of NK cells for efficient target cell cytolysis. Previously when NK cells were exploited for immunotherapy in this tumor model, repetitive conditioning of mice with an IL2 superkine (H9) resulted in a slight delay in tumor outgrowth, however, most of mice still had to be sacrificed within 35 days after tumor inoculation (12). In another study, effective control of RMA-S tumors required the transfer of high numbers of *in vitro* pre-activated NK cells and conditioning of mice by total body irradiation (11). In contrast to these studies, our protocol led to the induction of tumor-specific CD4$^+$ T cells, replacing the need for severe host conditioning and transfer of high numbers of cells. Although the exogenous IL2 in our protocol was not essential for the antitumor effect, it most likely supported complete tumor regressions (Supplementary Fig. S1A). IL2 support for NK cells appeared to be important in the mentioned previous reports, as exogenous cytokines or as produced by local CD4$^+$ T cells. Using OT2 transgenic mice, we showed that tumor-specific CD4$^+$ T cells, rather than any activated CD4$^+$ T cell, were required for the

Aldara-mediated control of tumors. This importance of antigen-specificity for the interplay of $CD4^+$ T cells with NK cells occurs in a *Leischmania major* infection model; antigen-specific $CD4^+$ T cells are required for NK cell activation in dLN (37). IL2 produced by $CD4^+$ T cells and IL12 produced by DCs are essential in inducing IFNγ-production by NK cells (37). These studies highlight the importance of IL2 in NK cell activation and suggest that the IL2 production by intratumoral $CD4^+$ T cells could be of importance in full NK cell function. Another mechanism by which tumor-specific $CD4^+$ T cells could mediate direct tumor control is through induction of tumor cell senescence through the production of cytokines intratumorally (38, 39).

Studies involving TLR7/8 agonists show that other immune cell types can mediate antitumor effects. In a B16 model, intratumoral injection of a TLR7/8 agonist results in suppression of tumor outgrowth of both injected as well as non-injected distal tumors, and this depends on the infiltration of M1-type macrophages, induced by CCL2 (40). Another study highlighted the role of plasmacytoid DCs in imiquimod-mediated regressions of melanomas (41). We depleted both pDCs and CSF1R macrophages, but this did not affect treatment outcome. Levels of CCL2 RNA were unchanged in $CD4^+$ T cell–depleted versus non-depleted tumors, indicating $CD4^+$ T cells were not involved in the induction of CCL2 in our model.

Patients who undergo treatment with checkpoint inhibitors or adoptive T-cell therapy have tumor-specific $CD4^+$ T cells, and their role in cancer therapeutics is beginning to be appreciated (42, 43). Our study underlines the central role of $CD4^+$ T cells as directors of the immune response in MHC-I^{low} cancers that escaped control by $CD8^+$ T cells, but become sensitive to NK cells. Vaccine-induced $CD4^+$ T cells interact with tumor-specific $CD8^+$ T cells in the MHC-I–proficient RMA lymphoma, showing that a broad immune response supported by T helper cells is key for the eradication of heterogeneous cancers, which usually have areas of MHC-I loss (24). Another study with MHC-II^{neg} plasmacytoma tumors highlighted the role $CD4^+$ T cells in macrophage-mediated tumor clearance (31, 44). Other tumor models support more efficient control of tumor outgrowth by $CD4^+$, rather than $CD8^+$, T cells (45). In a B16 melanoma model, adoptive cell transfer of tumor-specific $CD4^+$ T cells in combination with irradiation resulted in tumor regressions by direct killing of tumor cells by tumor-specific $CD4^+$ T cells (46). In another study with B16 tumors, $CD4^+$ T cells were involved in protection against tumor outgrowth after vaccination (32). Here, $CD4^+$ T cells were required for the infiltration of eosinophils, in line with our observation that $CD4^+$ T-cell–depleted tumors had reduced frequency of eosinophils. Together, these data reveal a central role for helper T cells in different immunotherapeutic approaches to cancer and confirm the importance of dedicated protocols that can effectively activate tumor-specific $CD4^+$ T cells. The crucial interplay between $CD4^+$ T cells and NK cells in the clearance of established MHC-I^{low} $MHCII^{neg}$ tumors might be exploited in future immunotherapies targeting immune-escaped tumors that are resistant to CD8 killer T cells.

Disclosure of Potential Conflicts of Interest

No potential conflicts of interest were disclosed.

Authors' Contributions

Conception and design: E.M. Doorduijn, R. Arens, F. Ossendorp, S.H. van der Burg, T. van Hall
Development of methodology: E.M. Doorduijn, D.C. Salvatori, S. Maas
Acquisition of data (provided animals, acquired and managed patients, provided facilities, etc.): E.M. Doorduijn, M. Sluijter
Analysis and interpretation of data (e.g., statistical analysis, biostatistics, computational analysis): E.M. Doorduijn, T. van Hall
Writing, review, and/or revision of the manuscript: E.M. Doorduijn, R. Arens, F. Ossendorp, S.H. van der Burg, T. van Hall
Administrative, technical, or material support (i.e., reporting or organizing data, constructing databases): M. Sluijter
Study supervision: F. Ossendorp, S.H. van der Burg, T. van Hall
Other (development execution and supervision of the histolopathology work): D.C. Salvatori
Other (Immunohistochemistry, pathology work): S. Silvestri

Acknowledgments

The authors would like to thank Marieke F. Fransen for useful discussions and Sjef Verbeek for providing the FcγR deficient mice.

Grant Support

This project was supported by the Dutch Cancer Society Fund (UL2010-4785) to T. van Hall and S.H. van der Burg.

The costs of publication of this article were defrayed in part by the payment of page charges. This article must therefore be hereby marked *advertisement* in accordance with 18 U.S.C. Section 1734 solely to indicate this fact.

Received November 21, 2016; revised April 12, 2017; accepted June 13, 2017; published OnlineFirst June 21, 2017.

References

1. Hodi FS, O'Day SJ, McDermott DF, Weber RW, Sosman JA, Haanen JB, et al. Improved survival with ipilimumab in patients with metastatic melanoma. N Engl J Med 2010;363:711–23.
2. Sharma P, Allison JP. Immune checkpoint targeting in cancer therapy: toward combination strategies with curative potential. Cell 2015;161:205–14.
3. Verdegaal EM, de Miranda NF, Visser M, Harryvan T, van Buuren MM, Andersen RS, et al. Neoantigen landscape dynamics during human melanoma-T cell interactions. Nature 2016;536:91–5.
4. Ferris RL, Whiteside TL, Ferrone S. Immune escape associated with functional defects in antigen-processing machinery in head and neck cancer. J Exp Med 2006;12:3890–5.
5. Carretero R, Romero JM, Ruiz-Cabello F, Maleno I, Rodriguez F, Camacho FM, et al. Analysis of HLA class I expression in progressing and regressing metastatic melanoma lesions after immunotherapy. Immunogenetics 2008;60:439–47.
6. Garrido F, Aptsiauri N, Doorduijn EM, Garcia Lora AM, van Hall T. The urgent need to recover MHC class I in cancers for effective immunotherapy. Curr Opin Immunol 2016;39:44–51.
7. Zaretsky JM, Garcia-Diaz A, Shin DS, Escuin-Ordinas H, Hugo W, Hu-Lieskovan S, et al. Mutations associated with acquired resistance to PD-1 blockade in melanoma. N Engl J Med 2016;375:819–29.
8. Ljunggren HG, Karre K. Host resistance directed selectively against H-2-deficient lymphoma variants. Analysis of the mechanism. J Exp Med 1985;162:1745–59.
9. Karre K, Ljunggren HG, Piontek G, Kiessling R. Selective rejection of H-2-deficient lymphoma variants suggests alternative immune defence strategy. Nature 1986;319:675–8.
10. Parkhurst MR, Riley JP, Dudley ME, Rosenberg SA. Adoptive transfer of autologous natural killer cells leads to high levels of circulating natural killer cells but does not mediate tumor regression. Clin Cancer Res 2011;17:6287–97.

11. Ni J, Miller M, Stojanovic A, Garbi N, Cerwenka A. Sustained effector function of IL-12/15/18-preactivated NK cells against established tumors. J Exp Med 2012;209:2351–65.
12. Ardolino M, Azimi CS, Iannello A, Trevino TN, Horan L, Zhang L, et al. Cytokine therapy reverses NK cell anergy in MHC-deficient tumors. J Clin Invest 2014;124:4781–94.
13. Wiedemann GM, Jacobi SJ, Chaloupka M, Krachan A, Hamm S, Strobl S, et al. A novel TLR7 agonist reverses NK cell anergy and cures RMA-S lymphoma-bearing mice. Oncoimmunology 2016;5:e1189051.
14. Chow LQ, Morishima C, Eaton KD, Baik CS, Goulart BH, Anderson LN, et al. Phase 1b trial of the toll-like receptor 8 agonist, motolimod (VTX-2337), combined with cetuximab in patients with recurrent or metastatic SCCHN. Clin Cancer Res 2017;23:2442–50.
15. Belani CP, Chakraborty B, Modi R, Khamar B. A Randomized Trial of TLR-2 agonist CADI-05 targeting desmocollin-3 for advanced non-small-cell lung cancer. Ann Oncol 2016;28:298–304.
16. Weihrauch MR, Richly H, von Bergwelt-Baildon MS, Becker HJ, Schmidt M, Hacker UT, et al. Phase I clinical study of the toll-like receptor 9 agonist MGN1703 in patients with metastatic solid tumours. Eur J Cancer 2015;51:146–56.
17. van Hall T, Wolpert EZ, van Veelen P, Laban S, van der Veer M, Roseboom M, et al. Selective cytotoxic T-lymphocyte targeting of tumor immune escape variants. Nat Med 2006;12:417–24.
18. Lampen MH, van Hall T. Strategies to counteract MHC-I defects in tumors. Curr Opin Immunol 2011;23:293–8.
19. Seidel UJ, Oliveira CC, Lampen MH, Hall T. A novel category of antigens enabling CTL immunity to tumor escape variants: Cinderella antigens. Cancer Immunol Immunother 2012;61:119–25.
20. Oliveira CC, Querido B, Sluijter M, de Groot AF, van der Zee R, Rabelink MJ, et al. New role of signal peptide peptidase to liberate C-terminal peptides for MHC class I presentation. J Immunol 2013;191:4020–8.
21. Doorduijn EM, Sluijter M, Querido BJ, Oliveira CC, Achour A, Ossendorp F, et al. TAP-independent self-peptides enhance T cell recognition of immune-escaped tumors. J Clin Invest 2016;126:784–94.
22. Ho NI, Camps MGM, de Haas EFE, Trouw LA, Verbeek JS, Ossendorp F. C1q-dependent dendritic cell cross-presentation of in vivo-formed antigen-antibody complexes. J Immunol 2017;198:4235–43.
23. van der Sluis TC, Sluijter M, van Duikeren S, West BL, Melief CJ, Arens R, et al. Therapeutic peptide vaccine-induced CD8 T cells strongly modulate intratumoral macrophages required for tumor regression. Cancer Immunol Res 2015;3:1042–51.
24. Ossendorp F, Mengede E, Camps M, Filius R, Melief CJ. Specific T helper cell requirement for optimal induction of cytotoxic T lymphocytes against major histocompatibility complex class II negative tumors. J Exp Med 1998;187:693–702.
25. Welten SP, Redeker A, Franken KL, Oduro JD, Ossendorp F, Cicin-Sain L, et al. The viral context instructs the redundancy of costimulatory pathways in driving CD8(+) T cell expansion. eLife 2015;4. doi: 10.7554/eLife.07486.
26. Walter A, Schafer M, Cecconi V, Matter C, Urosevic-Maiwald M, Belloni B, et al. Aldara activates TLR7-independent immune defence. Nat Commun 2013;4:1560.
27. Glas R, Waldenstrom M, Hoglund P, Klein G, Karre K, Ljunggren HG. Rejection of tumors in mice with severe combined immunodeficiency syndrome determined by the major histocompatibility complex. Class I expression on the graft. Cancer Res 1995;55:1911–6.
28. Adlard AL, Dovedi SJ, Telfer BA, Koga-Yamakawa E, Pollard C, Honeychurch J, et al. A novel systemically administered Toll-like receptor 7 agonist potentiates the effect of ionizing radiation in murine solid tumor models. Int J Cancer 2014;135:820–9.
29. Adams S, O'Neill DW, Nonaka D, Hardin E, Chiriboga L, Siu K, et al. Immunization of malignant melanoma patients with full-length NY-ESO-1 protein using TLR7 agonist imiquimod as vaccine adjuvant. J Immunol 2008;181:776–84.
30. Rechtsteiner G, Warger T, Osterloh P, Schild H, Radsak MP. Cutting edge: priming of CTL by transcutaneous peptide immunization with imiquimod. J Immunol 2005;174:2476–80.
31. Tveita AA, Schjesvold FH, Sundnes O, Haabeth OA, Haraldsen G, Bogen B. Indirect CD4+ T-cell-mediated elimination of MHC II(NEG) tumor cells is spatially restricted and fails to prevent escape of antigen-negative cells. Eur J Immunol 2014;44:2625–37.
32. Hung K, Hayashi R, Lafond-Walker A, Lowenstein C, Pardoll D, Levitsky H. The central role of CD4(+) T cells in the antitumor immune response. J Exp Med 1998;188:2357–68.
33. Wennerberg E, Kremer V, Childs R, Lundqvist A. CXCL10-induced migration of adoptively transferred human natural killer cells toward solid tumors causes regression of tumor growth in vivo. Cancer Immunol Immunother 2015;64:225–35.
34. Wendel M, Galani IE, Suri-Payer E, Cerwenka A. Natural killer cell accumulation in tumors is dependent on IFN-gamma and CXCR3 ligands. Cancer Res 2008;68:8437–45.
35. Pak-Wittel MA, Yang L, Sojka DK, Rivenbark JG, Yokoyama WM. Interferon-gamma mediates chemokine-dependent recruitment of natural killer cells during viral infection. Proc Nat Acad Sci U S A 2013;110:E50–9.
36. Stojanovic A, Cerwenka A. Natural killer cells and solid tumors. J Innate Immun 2011;3:355–64.
37. Bihl F, Pecheur J, Breart B, Poupon G, Cazareth J, Julia V, et al. Primed antigen-specific CD4+ T cells are required for NK cell activation in vivo upon Leishmania major infection. J Immunol 2010;185:2174–81.
38. Braumuller H, Wieder T, Brenner E, Assmann S, Hahn M, Alkhaled M, et al. T-helper-1-cell cytokines drive cancer into senescence. Nature 2013;494:361–5.
39. Kang TW, Yevsa T, Woller N, Hoenicke L, Wuestefeld T, Dauch D, et al. Senescence surveillance of pre-malignant hepatocytes limits liver cancer development. Nature 2011;479:547–51.
40. Singh M, Khong H, Dai Z, Huang XF, Wargo JA, Cooper ZA, et al. Effective innate and adaptive antimelanoma immunity through localized TLR7/8 activation. J Immunol 2014;193:4722–31.
41. Palamara F, Meindl S, Holcmann M, Luhrs P, Stingl G, Sibilia M. Identification and characterization of pDC-like cells in normal mouse skin and melanomas treated with imiquimod. J Immunol 2004;173:3051–61.
42. Kitano S, Tsuji T, Liu C, Hirschhorn-Cymerman D, Kyi C, Mu Z, et al. Enhancement of tumor-reactive cytotoxic CD4+ T cell responses after ipilimumab treatment in four advanced melanoma patients. Cancer Immunol Res 2013;1:235–44.
43. Linnemann C, van Buuren MM, Bies L, Verdegaal EM, Schotte R, Calis JJ, et al. High-throughput epitope discovery reveals frequent recognition of neo-antigens by CD4+ T cells in human melanoma. Nat Med 2015;21:81–5.
44. Haabeth OA, Tveita AA, Fauskanger M, Schjesvold F, Lorvik KB, Hofgaard PO, et al. How Do CD4(+) T cells detect and eliminate tumor cells that either lack or express MHC Class II Molecules? Front Immunol 2014;5:174.
45. Perez-Diez A, Joncker NT, Choi K, Chan WF, Anderson CC, Lantz O, et al. CD4 cells can be more efficient at tumor rejection than CD8 cells. Blood 2007;109:5346–54.
46. Quezada SA, Simpson TR, Peggs KS, Merghoub T, Vider J, Fan X, et al. Tumor-reactive CD4(+) T cells develop cytotoxic activity and eradicate large established melanoma after transfer into lymphopenic hosts. J Exp Med 2010;207:637–50.